[3Fe-4S] Clusters

DOI: 10.1002/anie.200900548

Structure of Active IspH Enzyme from *Escherichia coli* Provides Mechanistic Insights into Substrate Reduction**

Tobias Gräwert, Felix Rohdich, Ingrid Span, Adelbert Bacher, Wolfgang Eisenreich, Jörg Eppinger,* and Michael Groll**

Eukaryotes and most prokaryotes require isopentenyl diphosphate (IPP) and dimethylallyl diphosphate (DMAPP) as biosynthetic precursors of terpenes. Whereas animals generate these essential metabolites via the mevalonate pathway,[1] many human pathogens including *Plasmodium falciparum* and *Mycobacterium tuberculosis* are known to use the more recently identified non-mevalonate pathway, which is a potential target for drug development.[2–4] The final step of this pathway is catalyzed by IspH protein, which generates a mixture of IPP and DMAPP by reductive dehydration of 1-hydroxy-2-methyl-2-(*E*)-butenyl-4-diphosphate (HMBPP, Figure 1 a).[5–11] Recently, Rekittke et al. described the first X-ray structure of IspH protein from the hyperthermophilic eubacterium *Aquifex aeolicus* in its open state.[12] Herein, we report the crystal structure of the IspH protein from *Escherichia coli*[11] in its closed conformation, which serves as basis for a detailed discussion of the catalytic pathway.

Recombinant *E. coli* IspH protein (comprising an N-terminal His_6 fusion tag) was purified and crystallized under anaerobic conditions. Its structure was determined to a resolution of 1.8 Å by single-wavelength anomalous diffraction methods. Three iron sites per protein unit were localized in the anomalous difference Patterson map and were used for phasing. Successive rounds of model building and refinement afforded a well-defined electron density for the entire IspH molecule except for the N-terminal His_6 tag and five C-terminal amino acid residues ($R_{free} = 23.8\,\%$, Supporting Information, Table S2). The root mean square (r.m.s.) deviation between the C_α positions of the two protein molecules in the asymmetric unit is less than 0.3 Å.

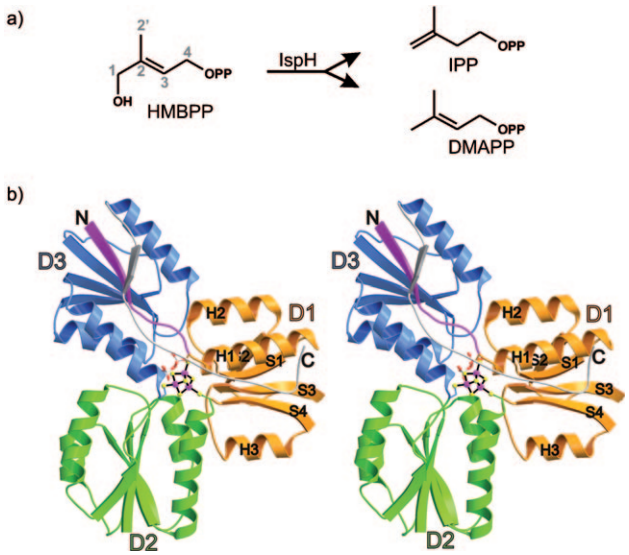

Figure 1. a) Reaction catalyzed by IspH. b) Crystal structure of *E. coli* IspH as ribbon drawing (stereoview) including numbering of domains, helices, and strands. The N-terminal strand S4 (purple) plays a key role for structural cohesion; protein data base (pdb) code: 3F7T.

The folding pattern of the monomeric protein involves three structurally similar domains, D1 to D3, which are related by pseudo-C_3 symmetry but are devoid of detectable sequence similarity (Figure 1 b and Supporting Information, Figure S1). Relative to domain D1, domains D2 and D3 appear rotated by angles of approximately 100° and 140°, respectively. Each domain starts with a conserved cysteine residue that protrudes into a cavity at the center of the protein where it coordinates one respective iron atom of a [3Fe-4S] cluster. The cluster appears to be tilted relative to the pseudo-trigonal axis of the apoprotein by about 20°. The trigonal symmetric [3Fe-4S] cluster is located in a hydrophobic pocket of the central cavity, which is formed by residues located on D1 (G14 and V15), D2 (P97 and V99), D3 (A199) as well as the C-terminus (F302 and P305), which stabilizes the arrangement of the individual domains. Furthermore, the methylene moiety of C96 in D2 is turned inward generating additional hydrophobic shielding of atom Fe^2 (see Figure 2).

Residual electron density located inside the central cavity was identified as inorganic diphosphate (PP_i; see Supporting

[*] Dr. T. Gräwert, Dr. F. Rohdich, I. Span, Prof. A. Bacher, Prof. W. Eisenreich, Prof. M. Groll
Center for Integrated Protein Science, Lehrstuhl für Biochemie
Department Chemie, Technische Universität München
Lichtenbergstrasse 4, 85747 Garching (Germany)
Fax: (+49) 89-2891-3363
E-mail: tobias.graewert@ch.tum.de
michael.groll@ch.tum.de
Dr. J. Eppinger
Department Chemie
Technische Universität München (Germany)
Current address:
King Abdullah University of Science and Technology
KAUST Catalysis Center, Thuwal (Saudi Arabia)
E-mail: joerg.eppinger@ch.tum.de
Joerg.Eppinger@KAUST.edu.sa

[**] We are grateful to Matthias Lee for developing the enzymatic assay, to Claudia Baier for recording cyclic voltammograms and to the staff of PXII at the Swiss Light Source (Villigen), in particular Clemens Schulze-Briese, for help during data collection. We thank the Hans-Fischer Gesellschaft and the Stifterverband für die Deutsche Wissenschaft (Projekt-Nr. 11047: Forschungsdozentur Molekulare Katalyse) for financial support.

Supporting information for this article is available on the WWW under http://dx.doi.org/10.1002/anie.200900548.

Information, Figure S3 for omit map; notably, the equilibrium concentration of diphosphate in the crystallization buffer is in the micromolar range[13,14]). The diphosphate is embedded in a hydrogen-bonding network involving several conserved amino acid residues (E126, T167, N227, histidines 41, 74, and 124, serines 225, 226, and 269, Figure 2; see Supporting

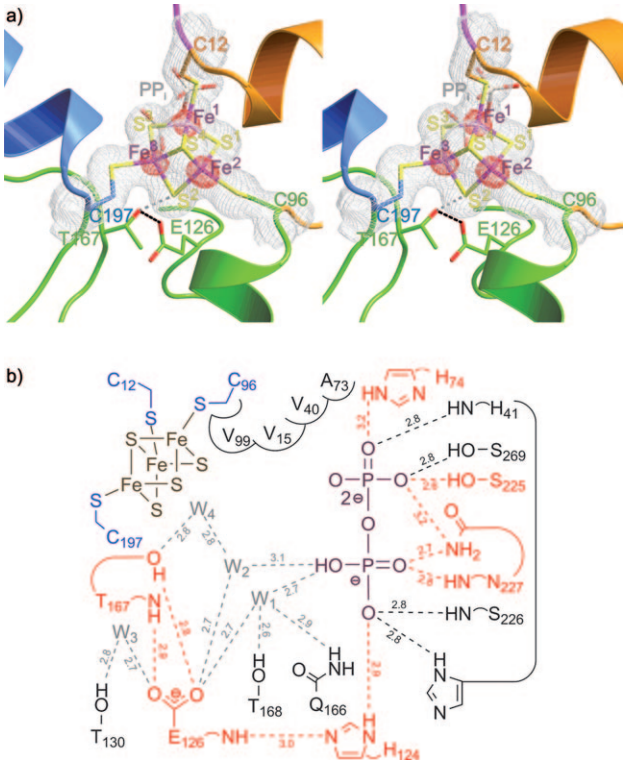

Figure 2. Active site of *E. coli* IspH. a) Electron density represented in gray is contoured at 1.0 σ with $2F_0$-F_c coefficients (stereoview). Color coding and orientation are identical to Figure 1b. The anomalous electron density identifying the individual iron sites is contoured at 25 σ (red). b) Representation of the coordinated PP_i with the anticipated hydrogen-bonding network indicated by dashed lines. Depicted amino acids are stringently conserved. Red: At least one mutation results in loss of activity. For structural orientation of key residues, see the Supporting Information, Figure S3.

Information, Figure S2 for sequence alignment). Whereas H41 or H74 can be replaced by asparagine with relative impunity, the activity of a H124N mutant was below detection level. S225C, N227Q, E126D, and E126Q mutations each afforded soluble protein with low or undetectable activity. Replacement of H41, H74, or H124 by alanine or replacement of T167 by asparagine or valine afforded insoluble protein (Supporting Information, Table S1). Replacement of V99 by alanine did not affect catalytic activity. Earlier studies have established that each of the cysteine residues coordinating the iron–sulfur cluster is essential.[11]

Various additives modulate the enzymatic activity (Supporting Information, Figure S7, Table S1). Diphosphate (c-(PP_i) = 10 mM) reduces activity to 28 ± 5% whereas orthophosphate buffer causes only slight inhibition (62 ± 8% residual activity for $c(P_i)$ = 900 mM). In the presence of 10 mM product IPP, activity is reduced to roughly half of the original value. To answer the question, whether the [3Fe-4S] cluster found in the crystal structure represents the active cofactor or just a degradation product of an aconitase-like [4Fe-4S] cluster,[5,6,12] we conducted activity studies in the presence of 0.5 mM Fe^{II}. Interestingly, a decreased activity (77 ± 8%) is evident under such conditions. On the other hand, a solution obtained by dissolving IspH protein crystals showed about 70 ± 25% enzyme activity as monitored by photometric as well as NMR-spectroscopy-based assays despite the presence of inhibiting phosphate (90 mM, from crystallization buffer) and bound PP_i. In agreement with earlier enzymatic and EPR-spectroscopic studies,[11] these findings confirm the [3Fe-4S] cluster as catalytically competent cofactor of the active enzyme.

Computer-assisted docking afforded the substrate conformation shown in Figure 3 to be preferred by at least 38 kJ mol^{-1} over any other binding mode tested (Supporting Information, Figure S8, Table S3). For this quasi-cyclic con-

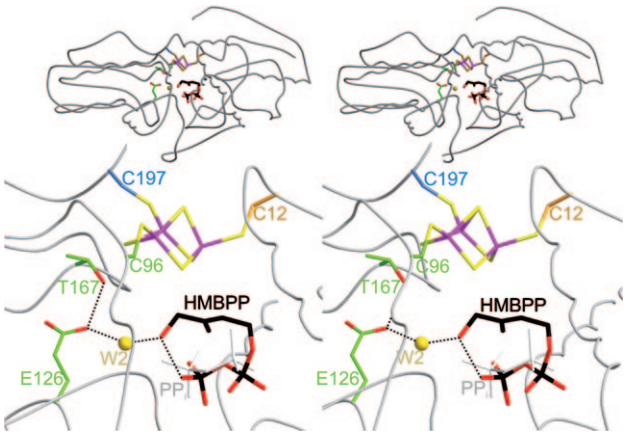

Figure 3. Stereoview of active site with bound HMBPP (black) in quasi-cyclic conformation including bound water W2 (yellow, see Supporting Information 2.8.2. for influence of water on docking results) as calculated by MD simulations; PP_i (gray, crystallographic data).

formation, the orientation of the HMBPP diphosphate moiety corresponds well to that of the PP_i ligand present in the crystal structure.[15] Carbon atoms 1 to 3 of the allylic system are situated on the open face of the iron–sulfur cluster with the methyl carbon C-2′ pointing into a hydrophobic pocket. The quasi-cyclic substrate conformation is stabilized by a hydrogen bond between the acidic proton of the diphosphate moiety and the oxygen of the allylic alcohol proximate to E126. Quantum chemical assessments of potential reaction intermediates and transition states provide further insights into the mechanism of the IspH-catalyzed reductive dehydroxylation (see Supporting Information 2.8 for details). For a $[HMBPP(H^+)]^{3-}$ radical ($S = {}^1/_2$) in the cyclic confirmation, which represents the first intermediate after initial electron transfer, we could not locate a minimum species on the potential surface. During minimization C(4)–O bond rupture occurs, leading to a C(2)-C(3)-C(4) allylic radical and a double-protonated PP_i. This result is in agreement with the notion, that PP_i is a better leaving group than a

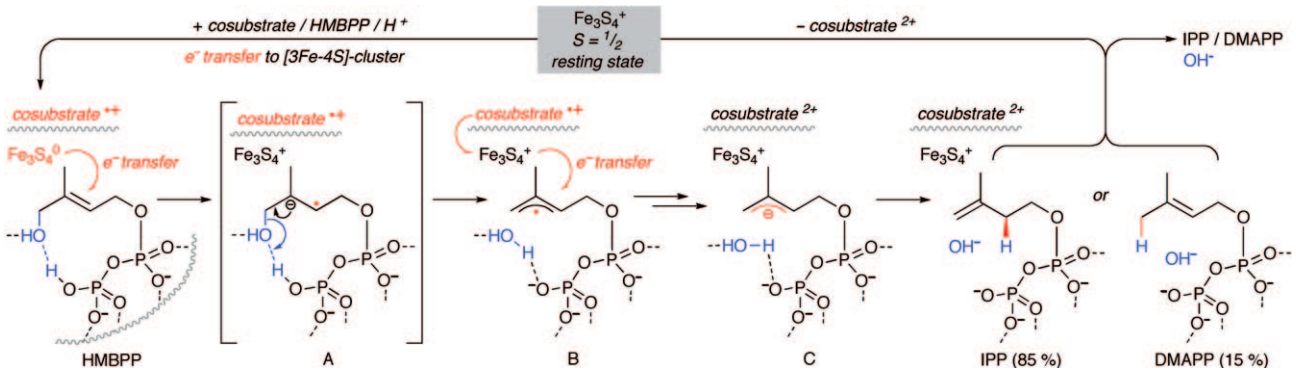

Scheme 1. Suggested sequence of electron and proton transfer during the IspH-catalyzed reduction of HMBPP to IPP/DMAPP. Gray waved lines indicate the rim of the cavity containing the active site. The biological cosubstrate of IspH is flavodoxin. Charges of the intermediate iron–sulfur clusters are in agreement with data from [3Fe-4S] clusters of other proteins[22] as well as model systems.[23]

hydroxy moiety. However, after constraining the C(4)–O bond to 1.47 Å, minimization leads to cleavage of the C(1)–O bond yielding a C(1)-C(2)-C(3) allylic radical intermediate and a water molecule. This pathway corresponds to formation of intermediate B in Scheme 1. Labilization of the C–O bond by a neighboring delocalized radical anion resembles the situation in ribonucleotide reductase or 2-hydroxyglutaryl-CoA dehydratase, where elimination of a α-hydroxy group has been demonstrated to occur from a ketyl-like radical intermediate (Supporting Information, Figure S9).

Since the electrochemical potential of the [3Fe-4S] core ($E^{0\prime} = -0.25$ V)[16] does not allow electron transfer to allylic alcohols ($E^{0\prime} = -1.25$ V),[17] activation of HMBPP by the protein environment is proposed to be the crucial step in initiating substrate reduction. Based on the crystal structure and on molecular dynamics (MD) simulations, a Lewis acid activation by one of the iron centers[12] can be ruled out because of steric shielding. However, the cyclic conformation of the bound substrate favors a hydrogen bond between the alcohol function and the Brønsted acidic diphosphate OH moiety. Proton transfer from the diphosphate moiety to the alcohol group of HMBPP may be induced by a combination of several effects. The location of the diphosphate binding site at the positively charged N-terminus of three α-helical H2 units (one from each domain) leads to an increased acidity of the surrounding polar side-chain residues and destabilizes protonation of the diphosphate. Moreover, the negative charge on E126 stabilizes a positive charge on the proximate allylic OH moiety. These factors may trigger one-electron transfer followed by the allylic C–O bond rupture described above. For IspH, geometric constraints induced by the enzyme's cavity prevent the loss of the diphosphate (PP_i) moiety and lead to elimination of the hydrogen bonded OH^- instead.

Protonation of the allyl anion (C in Scheme 1), probably employing water as proton source, has to occur from the diphosphate side (H^{Si}-side), since the opposite face of the allylic system is blocked by the lipophilic surface of the [3Fe-4S] cluster. This situation is in agreement with the observed stereochemistry of the reaction.[18] The product ratio of IPP and DMAPP is kinetically controlled (preferential protonation at C-3).[19] The increased negative charge inside the binding pocket resulting from the consecutive injection of two electrons could trigger product release.

Superposition of the crystal structures of IspH protein from *E. coli* and *A. aeolicus* reveals a significant opening of the central cavity for the *A. aeolicus* enzyme, which is induced by a tilt of Domain D3 by about 20° with respect to Domains D1 and D2 (see Supporting Information, Figure S10 for C_α superposition). This change in tertiary structure can be traced to dihedral angle differences involving amino acids R9-G10-F11 from *E. coli* and A10-G11-F12 from *A. aeolicus* and from C197 (*E. coli*) and C193 (*A. aeolicus*) which may constitute a dynamic hinge enabling the opening and closing of the active site cavity. Mutational studies suggest that this motion is induced by binding of the PP_i ligand at the conserved SXN motif in D3 (S225-S226-N227 in *E. coli*; S221-G222-N223 in *A. aeolicus*), rather than by interaction with the histidine residues H41 and H74 (*E. coli*) or H42 and H74 (*A. aeolicus*). Movement of the relevant amino acids is depicted in Figure 4.

In conclusion, we present a structure-based rationale of the substrate binding mode, which in combination with mutational studies and theoretical calculation supports a reaction mechanism representing a biological counterpart of the Birch reduction of allylic alcohols with lithium in liquid ammonia.[10] The binding and activation of HMBPP-substrate significantly differ from recent proposals.[5,6,12] Since enzymes of the non-mevalonate pathway include predicted[20] or

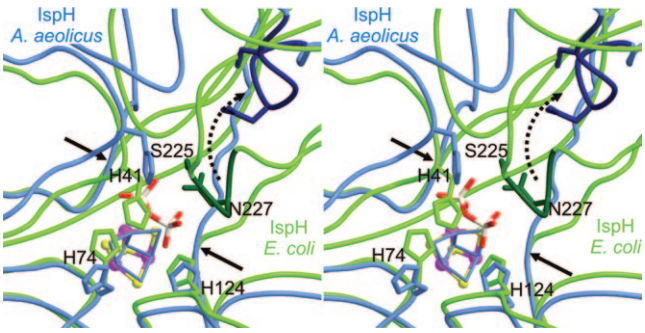

Figure 4. Superposition (stereoview) of IspH protein from *E. coli* (green, closed conformation) and *A. aeolicus* (blue; open conformation). The dashed arrow symbolizes the movement of the SXN loop, solid arrows indicate positions of the hinge motifs of D3.

clinically validated[21] targets for drug development, our studies may trigger the design of new antimicrobial substances qualifying for the treatment of several pandemic diseases.

Received: January 29, 2009
Revised: March 25, 2009
Published online: June 30, 2009

Keywords: iron–sulfur clusters · enzymes · isoprenes · non-mevalonate pathway · reaction mechanisms

[1] K. Bloch, *Steroids* **1992**, *57*, 378 – 383.
[2] M. Rohmer, M. Knani, P. Simonin, B. Sutter, H. Sahm, *Biochem. J.* **1993**, *295*, 517 – 524.
[3] H. P. Kuemmerle, T. Murakawa, H. Sakamoto, N. Sato, T. Konishi, F. De Santis, *Int. J. Clin. Pharmacol. Ther. Toxicol.* **1985**, *23*, 521 – 528.
[4] H. Jomaa, J. Wiesner, S. Sanderbrand, B. Altincicek, C. Weidemeyer, M. Hintz, I. Türbachova, M. Eberl, J. Zeidler, H. Lichtenthaler, D. Soldati, E. Beck, *Science* **1999**, *285*, 1573 – 1576.
[5] M. Wolff, M. Seemann, B. T. Sim, Y. Frapart, D. Tritsch, A. G. Estrabot, M. Rodríguez-Concepción, A. Boronat, A. Marquet, M. Rohmer, *FEBS Lett.* **2003**, *541*, 115 – 120.
[6] B. Altincicek, E. C. Duin, A. Reichenberg, R. Hedderich, A.-K. Kollas, M. Hintz, S. Wagner, E. Beck, H. Jomaa, *FEBS Lett.* **2003**, *532*, 437 – 440.
[7] Y. Xiao, Z. K. Zhao, P. Liu, *J. Am. Chem. Soc.* **2008**, *130*, 2164 – 2165.
[8] Y. Xiao, P. Liu, *Angew. Chem.* **2008**, *120*, 9868 – 9871; *Angew. Chem. Int. Ed.* **2008**, *47*, 9722 – 9725.
[9] F. Rohdich, S. Hecht, K. Gärtner, P. Adam, C. Krieger, S. Amslinger, D. Arigoni, A. Bacher, W. Eisenreich, *Proc. Natl. Acad. Sci. USA* **2002**, *99*, 1158 – 1163.
[10] F. Rohdich, F. Zepeck, P. Adam, S. Hecht, J. Kaiser, R. Laupitz, T. Gräwert, S. Amslinger, W. Eisenreich, A. Bacher, D. Arigoni, *Proc. Natl. Acad. Sci. USA* **2003**, *100*, 1586 – 1591.
[11] T. Gräwert, J. Kaiser, F. Zepeck, R. Laupitz, S. Hecht, S. Amslinger, N. Schramek, E. Schleicher, S. Weber, M. Haslbeck, J. Buchner, C. Rieder, D. Arigoni, A. Bacher, W. Eisenreich, F. Rohdich, *J. Am. Chem. Soc.* **2004**, *126*, 12847 – 12855.
[12] I. Rekittke, J. Wiesner, R. Rohdich, U. Demmer, E. Warkentin, W. Xu, K. Troschke, M. Hintz, J. H. No, E. C. Duin, E. Oldfield, H. Jomaa, U. Ermler, *J. Am. Chem. Soc.* **2008**, *130*, 17206 – 17207.
[13] H. Floodgard, P. Fleron, *J. Biol. Chem.* **1974**, *249*, 3465 – 3474.
[14] Crystallization of IspH from phosphate-free 1.5 M malonate buffer (pH 6.5) resulted in a nearly identical protein structure, with the PP_i ligand being replaced by malonate occupying the same binding location (Supporting Information, Figure S5 and S6).
[15] The binding mode of PP_i may generally be indicative for the location of diphosphate residues of substrates in the binding pocket (Supporting Information, Figure S4).
[16] The cyclic voltammogram exhibits a reversible one electron reduction wave at $E^{0\prime} = -0.25$ V and an irreversible two electron reduction wave at $E^{0\prime} = -0.58$ V, which is typical for [3Fe-4S] proteins: J. N. Butt, F. A. Armstrong, J. Breton, S. J. George, A. J. Thomson, E. C. Hatchikian, *J. Am. Chem. Soc.* **1991**, *113*, 6663 – 6670.
[17] H. Shukun, S. Souqun, S. Jian, *J. Org. Chem.* **2001**, *66*, 4487 – 4493.
[18] R. Laupitz, T. Gräwert, C. Rieder, F. Zepeck, A. Bacher, D. Arigoni, F. Rohdich, W. Eisenreich, *Chem. Biodiversity* **2004**, *1*, 1367 – 1376.
[19] P. Adam, S. Hecht, W. Eisenreich, J. Kaiser, T. Gräwert, D. Arigoni, A. Bacher, F. Rohdich, *Proc. Natl. Acad. Sci. USA* **2002**, *99*, 12108 – 12113.
[20] W. Eisenreich, A. Bacher, D. Arigoni, F. Rohdich, *Cell. Mol. Life Sci.* **2004**, *61*, 1401 – 1426.
[21] M. A. Missinou, S. Borrmann, A. Schindler, S. Issifou, A. A. Adegnika, P. B. Matsiegui, R. Binder, B. Lell, J. Wiesner, T. Baranek, H. Jomaa, P. G. Kremsner, *Lancet* **2002**, *360*, 1941 – 1942.
[22] M. K. Johnson, *Curr. Opin. Chem. Biol.* **1998**, *2*, 173 – 181, and references therein.
[23] P. W. Rao, R. H. Holm, *Chem. Rev.* **2004**, *104*, 527 – 560.

